

ChemComm

Accepted Manuscript



This is an *Accepted Manuscript*, which has been through the Royal Society of Chemistry peer review process and has been accepted for publication.

Accepted Manuscripts are published online shortly after acceptance, before technical editing, formatting and proof reading. Using this free service, authors can make their results available to the community, in citable form, before we publish the edited article. We will replace this *Accepted Manuscript* with the edited and formatted *Advance Article* as soon as it is available.

You can find more information about *Accepted Manuscripts* in the [Information for Authors](#).

Please note that technical editing may introduce minor changes to the text and/or graphics, which may alter content. The journal's standard [Terms & Conditions](#) and the [Ethical guidelines](#) still apply. In no event shall the Royal Society of Chemistry be held responsible for any errors or omissions in this *Accepted Manuscript* or any consequences arising from the use of any information it contains.

COMMUNICATION

Immobilization of Polyoxometalates in the Zr-based Metal Organic Framework UiO-67

Cite this: DOI: 10.1039/x0xx00000x

William Salomon,^a Catherine Roch-Marchal,^{*a} Pierre Mialane,^a Paul Rouschmeyer,^a Christian Serre,^a Mohamed Haouas,^a Francis Taulelle,^a Shu Yang,^b Laurent Ruhlmann^b and Anne Dolbecq^{*a}

Received 00th January 2012,

Accepted 00th January 2012

DOI: 10.1039/x0xx00000x

www.rsc.org/

The encapsulation of polyoxometalates within the large pores of the Zr(IV) biphenyldicarboxylate UiO-67 metal-organic framework has been achieved, for the first time, by direct solvothermal synthesis. The resulting POM@UiO-67 composite materials were fully characterized by XRPD, IR, MAS NMR, N₂ porosimetry measurements and cyclic voltammetry.

Polyoxometalates (POMs) are soluble early-transition-metal clusters with a large diversity of structures and compositions.¹ They possess redox and acid-base properties which can be exploited for catalytic applications.² However their low specific surface area, low stability under catalytic conditions and high solubility in aqueous solution constitute some of their drawbacks. The search for stable heterogeneous catalysts with high surface area, which could combine the activity of the POMs with the advantages of heterogeneous catalysts, such as an easier recovery and recycling thus attracts a lot of interest. Encapsulation of POMs within the cavities of metal organic frameworks (MOFs)³ constitutes one strategy to access to POMs-based heterogeneous catalysts.⁴ The mesoporous M(III)-trimesate MIL-100 and -terephthalate MIL-101 families (M = Fe, Cr, Al; MIL stands for Material of Institut Lavoisier) have been the most investigated host matrices so far because of their very large pore sizes and surface areas and good chemical stability. Keggin-type as well as sandwich-type POMs have been incorporated either by impregnation or *in situ* during the MOF synthesis.⁵ Besides the MIL families, Cu-BTC frameworks (BTC = 1,3,5-benzenetricarboxylate), known as HKUST-1 (HKUST stands for Hong-Kong University of Science and Technology) have been the subject of intense researches.⁵ Due to the small size of the pores they can only accommodate Keggin anions by direct synthesis. However the poor aqueous stability of these copper carboxylate based MOFs might prevent from their practical use. Among the few examples of series of thermally, and chemically stable MOFs with high surface area, the UiO-66 to 68 family (UiO stands for University of Oslo), built up from {Zr^{IV}₆O₄(OH)₄} oxoclusters nodes and linear dicarboxylate linkers (with the general formulae [Zr^{IV}₆O₄(OH)₄(linker)₆]) is one of the most studied.⁶ These materials exhibit by themselves very promising catalytic properties.⁷ In UiO-67 the inorganic octahedral Zr₆ units are bound to 12 other inorganic

subunits through biphenyl dicarboxylate ligands forming a face-centered cubic (fcc) structure (a = 27.1 Å). This MOF exhibits two types of cages: supertetrahedral (∅ ~ 11.5 Å) and superoctahedral (∅ ~ 18 Å) accessible through microporous triangular windows (~ 8 Å) (Fig. 1a), corresponding to the voids of the fcc packing. However, the incorporation of guest molecules within the pores of UiO MOFs has only been rarely studied⁸ and, to our knowledge, there have been so far no report of POM@UiO composites. Here we propose for the first time a synthetic method for the encapsulation within the pores of UiO-67 of three representative examples of POMs: [PW₁₂O₄₀]³⁻, [PW₁₁O₃₉]⁷⁻ and [P₂W₁₈O₆₂]⁶⁻ which size (Fig. 1b-d) can fit in the microporous octahedral cavities of this MOF.

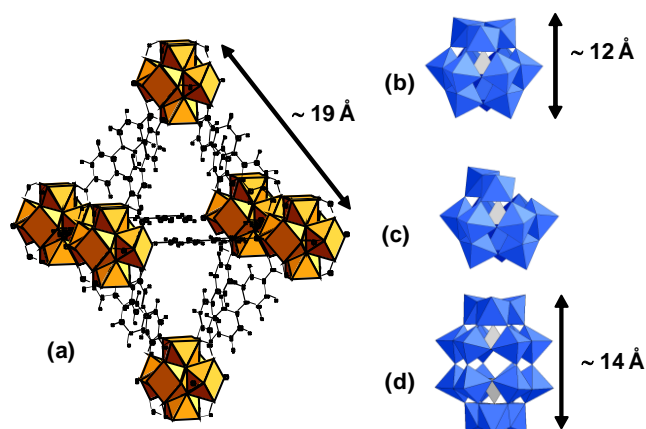


Fig. 1. Polyhedral representations of (a) the octahedral cages of UiO-67, (b) [PW₁₂O₄₀]³⁻ (PW₁₂), (c) [PW₁₁O₃₉]⁷⁻ (PW₁₁) and (d) [P₂W₁₈O₆₂]⁶⁻ (P₂W₁₈); blue octahedra: WO₆, grey tetrahedra: PO₄, orange polyhedra: ZrO₈, black spheres: C, small black spheres: H.

Attempts to incorporate POMs in the UiO-67 by an impregnation method, like for the MIL-101 materials,⁵ have failed. This can be related to the narrow size of the windows. Thus a direct synthesis approach has been considered. A mixture of the pre-formed POM species (H₃[PW₁₂O₄₀], TBA₄H₃[PW₁₁O₃₉] or TBA₆[P₂W₁₈O₆₂]), zirconium tetrachloride, benzoic acid as modulator,⁹ and

biphenyldicarboxylic acid was heated at 120 °C in dimethylformamide (DMF) (ESI†). Concentrated HCl was also added following previous reports.^{6b,d} One would also expect that in the synthetic conditions used for the synthesis of UiO-67, the monolacunary PW₁₁ POM would react with Zr(IV) ions to lead to the monomeric 1:1 complex [PW₁₁O₃₉Zr(H₂O)_n]³⁻ (n = 2, 3), postulated by Kholdeeva *et al.*¹⁰ Such monomeric monosubstituted complex has also been evidenced in the Dawson¹¹ and Lindquist family.¹² The resulting insoluble microcrystalline materials PW₁₂@UiO-67, PW₁₁Zr@UiO-67 and P₂W₁₈@UiO-67, respectively, were filtered and washed several times with DMF and acetone. Infrared (IR) spectra (Fig. 2) indicate both the presence of the POM and the MOF, with P-O and W-O vibration bands characteristic of the POM observed between 850 and 1100 cm⁻¹ together with the carboxylate vibration bands from the linker between 1300 and 1600 cm⁻¹. The positions of the Bragg peaks are similar in the X-ray powder diffraction pattern of bare UiO-67 and of the POM@UiO-67 materials, confirming that the introduction of POMs in the synthetic medium does not perturb the formation of the MOF (Fig. S1, ESI†).

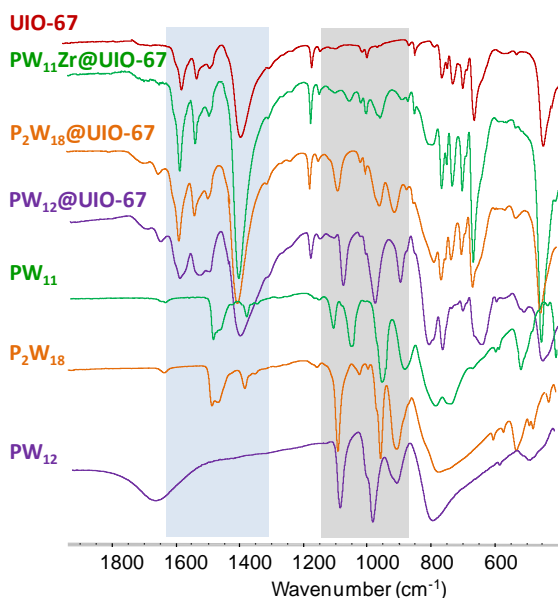


Fig. 2. IR spectra of POM@UiO-67 composites compared to that of the POM precursors and UiO-67. The regions with characteristic peaks of the POMs and of the MOF are highlighted in grey and light blue respectively.

Elemental analysis combined with thermogravimetric analysis (TGA) measurements allow proposing the [Zr₆O₄(OH)_{5.4}][C₁₄H₈O₄]_{5.3} formula for UiO-67, in agreement with the existence of linker defects occupied by hydroxide anions.^{6b} One expects that for the POM@UiO-67 composites, the negative charges introduced by the POMs compensate, almost totally, the linker deficiencies. Note that the presence of tetrabutylammonium cations can be ruled out both by IR, elemental analysis and nuclear magnetic resonance (NMR). The TGA curves for UiO-67 and its composites (Fig. S2 and Table S1, ESI†) reveal steps that are attributed to water removal, linker decomposition and formation of inorganic oxides. Combined with elemental analyses, these results lead to the estimation of the following formulae [Zr₆O₄(OH)₄][C₁₄H₈O₄]_{5.37}[PW₁₂O₄₀]_{0.42} (PW₁₂@UiO-67), [Zr₆O₄(OH)₄][C₁₄H₈O₄]_{5.73}[PW₁₁O₃₉Zr]_{0.18} (PW₁₁Zr@UiO-67), and [Zr₆O₄(OH)_{4.30}][C₁₄H₈O₄]_{5.10}[P₂W₁₈O₆₂]_{0.25} (P₂W₁₈@UiO-

67) for the POM@UiO-67 composites. As there is one octahedral cavity per Zr₆ unit, these formulae indicate that approximately 1/2, 1/5 and 1/4 of the cavities are occupied by POMs in PW₁₂@UiO-67, PW₁₁Zr@UiO-67 and P₂W₁₈@UiO-67, respectively.

N₂ sorption isotherms have been recorded for all the reported compounds (Fig. S3 and Table S2, ESI†). As expected, the surface area as well as the total pore volumes decrease from UiO-67 to POM@UiO-67 composites, as a consequence of the encapsulation of the POMs within the octahedral cavities, leaving however a significant porosity accessible to nitrogen. It should be noted that the values of the normalized specific surface area, taking into account the mass of UiO-67 in the composites samples, are significantly different from the value of UiO-67 (Fig. S3 and Table S2, ESI†), suggesting that the POMs are located inside the cavities and not at the surface of the material.

The ¹H MAS and ¹³C{¹H} CPMAS NMR spectra of the three POM@UiO-67 (Figs. S4-S5, ESI†) exhibit the characteristic resonances from the crystalline UiO-67. The Zr-OH hydroxyl protons from the hexameric unit lie in the 0-3.6 ppm range while the resonances of the linker, *i.e.* aromatic protons, are observed at 7.1 and 7.9 ppm. The aromatic carbon atoms (125, 130, 134, and 143 ppm) and the carbon atoms of the carboxylic function (172 ppm) are in the expected range.^{8c} Noteworthy, broad components of all these resonances are observed and the general tendency showed that higher the amount of encapsulated POM larger the fraction of these broad resonances (23% in PW₁₁Zr@UiO-67, 54% in P₂W₁₈@UiO-67, and 68% in PW₁₂@UiO-67). This is assigned to structural disorder caused by the POM filling pores.

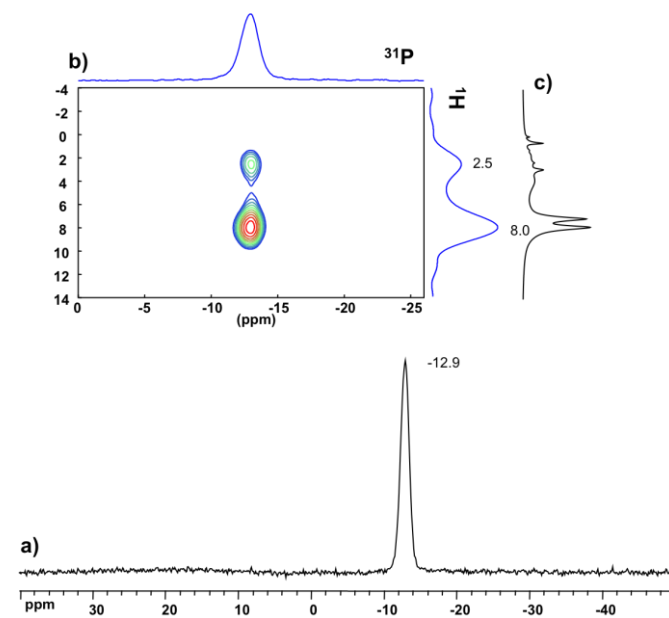


Fig. 3. Solid-state NMR spectra of P₂W₁₈@UiO-67: (a) ³¹P{¹H} CPMAS; (b) ¹H-³¹P HETCOR; (c) ¹H MAS.

The ³¹P MAS NMR spectra of PW₁₂@UiO-67 (Fig. S6a, ESI†) and P₂W₁₈@UiO-67 (Fig. 3a) show characteristic features of the POM precursors with signals at -15.2 and -12.9 ppm respectively, comparable to the literature values.¹³ In contrast, the spectrum of PW₁₁Zr@UiO-67 (Fig. S7a, ESI†) exhibits a resonance at -13.2 ppm instead of -12.4 ppm expected for

PW₁₁.¹⁴ This shift is in perfect agreement with that determined for a mixture of PW₁₁ and ZrCl₄ in DMF (Fig. S8, ESI†).

³¹P NMR provides not only information about the structure of the POM but also some insights on location and host-guest interactions between the POM and the MOF. Indeed, the ¹H-³¹P HETCOR (heteronuclear correlation) experiment enables to probe the dipolar contact between the ³¹P and ¹H nuclei. Correlations between the phosphorus site of the POM and protons of the aromatic linkers as well as Zr-OH framework hydroxyl groups are observed in the three POM@UiO-67 composite materials. This unambiguously indicates close proximity of the POM to the surface of the MOF inside the pores homogeneously as otherwise no such efficient dipolar transfer would be seen. Furthermore, the strength of the correlation with these protons appears contrasted from one POM to another. Indeed in P₂W₁₈@UiO-67 (Fig. 3b) and PW₁₂@UiO-67 (Fig. S6b, ESI†) the ³¹P site correlates mainly with the aromatic resonance (8 ppm) while in PW₁₁Zr@UiO-67 (Fig. S7b, ESI†) the correlation mainly occurs with the hydroxyl group peak (2.5 ppm). This clearly indicates preferential interaction of PW₁₂ and P₂W₁₈ with the organic linker, whereas PW₁₁Zr should be closer to the inorganic node, suggesting interactions between the Zr(IV) ions inserted in the POM lacuna and the {Zr^{IV}₆O₄(OH)₄} clusters. Finally, these correlations involve only the broad components of the ¹H spectra (as it could be compared with 1D MAS in Fig. 3c). This strongly suggests as stated above that the POMs are located in the distorted/disordered domain.

The electrochemical properties of the POM@UiO composite materials were also studied and compared to those of the POMs alone. The solids were first immobilized on the surface of the basal plane pyrolytic graphite disk (PG) and their electrochemical responses studied in pH 2.5 H₂SO₄/Na₂SO₄ 0.5 M buffer solutions. PW₁₂ and P₂W₁₈ and their related POM@UiO-67 composites exhibit similar redox behaviors related to the W^{V/IV} redox couples (Table S3, Figs. S9-S11, ESI† and Fig. 4), showing that when saturated POMs are encapsulated inside the cages they keep their electrochemical properties. It must be noted however that the first reduction process for P₂W₁₈ is 175 mV higher for P₂W₁₈@UiO-67 than for P₂W₁₈.

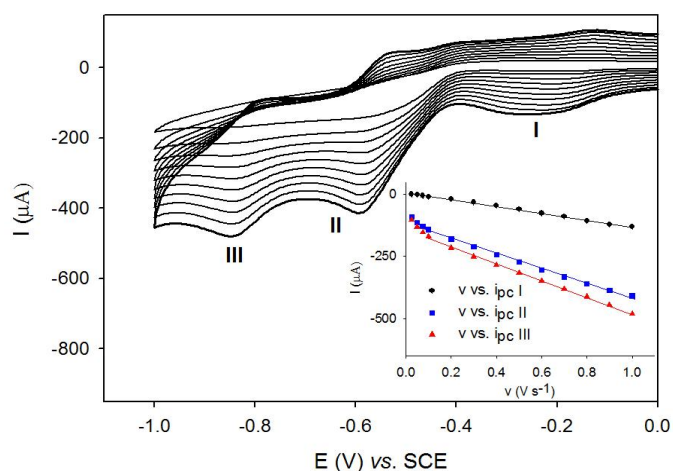


Fig. 4. Cyclic voltammograms of P₂W₁₈@UiO-67 immobilized at a PG electrode in a pH 2.5 H₂SO₄/Na₂SO₄ 0.5 M buffer solution at different scan rates from 0.025 to 1.000 V s⁻¹. Inset: plots of I_{pc} vs. v for peaks I, II and III.

In the case of PW₁₁Zr@UiO-67 the cyclic voltammogram clearly shows the complexation of the monolacunary PW₁₁ with Zr(IV) and the formation of PW₁₁Zr encapsulated in UiO-67 (Figs. S12-13, ESI†). Indeed, PW₁₁ immobilized on the PG exhibits four successive waves at -0.450 V, -0.560 V, -0.694 V and -0.830 V vs. SCE respectively while only two waves are measured for PW₁₁Zr@UiO-67 at -0.713V and -0.885 V. It should be noted that the electrochemical behaviors of the POM@UiO composites and of composites obtained by mechanical mixing of POMs and UiO (Fig. S14-S16) are different which confirm the encapsulation of the POMs inside the cavities and the transformation of PW₁₁ into PW₁₁Zr. Finally, all peak current intensities vary linearly with the scan rate in the range 0.1 V – 1.0 V s⁻¹, as expected for surface confined redox processes. This behavior is in agreement with the immobilization of the POMs inside the cavities of the MOF and contrasts with the observation of diffusion-controlled processes for PW₁₁@MIL-101(Cr) which were attributed to the mobility of the POMs.¹⁵

In conclusion, the immobilization of three polyoxotungstates in the largest pores of UiO-67(Zr) has been carried out for the first time, by a direct synthetic method. POM encapsulation compensates almost totally the linker deficiencies. The elaborated POM@UiO-67 composites have been thoroughly characterized. Cyclic voltammetry studies have confirmed the direct formation of PW₁₁Zr during the synthetic process and the integrity of the saturated inserted POMs PW₁₂ and P₂W₁₈. MAS NMR experiments have brought essential information on the structure of the composites. First, they have shown interactions between the POMs and the framework, thus confirming the encapsulation within the structure. Moreover they highlighted the existence of disordered domains related to the presence of the POMs. Finally they evidenced specific interactions between the asymmetric PW₁₁Zr POMs and the UiO framework. Noticeably, because of the small size of the cage windows, POM leaching cannot occur in these materials. The introduction of POMs might pave the way for future applications in catalysis. It may also greatly influence the hydrophilicity of the materials and thus their gas sorption properties. Future work will focus on these two applications.

This work was supported by CNRS, UVSQ, University of Strasbourg and the French National Research Agency (ANR) as part of the “Investissements d’Avenir” program n°ANR-11-IDEX-0003-02 and CHARMMMAT ANR-11-LABX-0039. Patricia Horcajada and Thomas Devic are gratefully acknowledged for fruitful discussions.

Notes and references

^a Institut Lavoisier de Versailles, UMR 8180, Université de Versailles Saint-Quentin en Yvelines, 45 Avenue des Etats-Unis, 78035 Versailles cedex, France. E-mail: catherine.roch@uvsq.fr (C.R.-M.), anne.dolbecq@uvsq.fr (A.D.)

^b Université de Strasbourg, Institut de Chimie, UMR CNRS 7177, Laboratoire d’Electrochimie et de Chimie Physique du Corps Solide, 4 rue Blaise Pascal, CS 90032, 67081 Strasbourg cedex, France.

†Electronic Supplementary Information (ESI) available: Detailed syntheses and characterizations. See DOI: 10.1039/c000000x/

1. (a) H. N. Miras, L. Vilà-Nadal and L. Cronin, *Chem. Soc. Rev.*, 2014, **43**, 5679; (b) O. Oms, A. Dolbecq and P. Mialane, *Chem. Soc. Rev.*, 2012, **41**, 7497; (c) A. Proust, B. Matt, R. Villanneau, G. Guillemot, P. Gouzerh and G. Izzet, *Chem. Soc. Rev.*, 2012, **41**, 7605.

2. (a) H. Lv, Y. V. Geletii, C. Zhao, J. W. Vickers, G. Zhu, Z. Luo, J. Song, T. Lian, D. G. Musaev, and C. L. Hill, *Chem. Soc. Rev.*, 2012, **41**, 7572; (b) A. Sartorel, M. Bonchio, S. Campagna and F. Scandola, *Chem. Soc. Rev.*, 2013, **42**, 2262; (c) N. Mizuno and K. Kamata, *Coord. Chem. Rev.*, 2011, **255**, 2358; (d) X.-B. Han, Z.-M. Zhang, T. Zhang, Y.-G. Li, W. Lin, W. You, Z.-M. Su, and E.-B. Wang, *J. Am. Chem. Soc.*, 2014, **136**, 5359.

3. *Chem. Soc. Rev.*, 2014, **43**, 5415, special issue on Metal Organic Frameworks.
4. J. Juan-Alcañiz, J. Gascon, and F. Kapteijn, *J. Mat. Chem.*, 2012, **22**, 10102.
5. See for example: (a) N. V. Maksimchuk, M. N. Timofeeva, M. S. Melgunov, A. N. Shmakov, Y. A. Chesalov, D. N. Dybtsev, V. P. Fedin and O. A. Kholdeeva, *J. Catal. A*, 2008, **257**, 315; (b) L. Bromberg, Y. Diao, H. Wu, S. C. A. Speakman and T. A. Hatton, *Chem. Mater.*, 2012, **24**, 1664; (c) C. M. Granadeiro, A. D. S. Barbosa, P. Silva, F. A. Almeida Paz, V. K. Saini, J. Pires, B. de Castro, S. S. Balula and L. Cunha-Silva, *Applied Catal. A: General*, 2013, **453**, 316; (d) J. Juan-Alcañiz, E. V. Ramos-Fernandez, U. Lafont, J. Gascon and F. Kapteijn, *J. Catal.*, 2010, **269**, 229; (e) A.-X. Yan, S. Yao, Y.-G. Li, Z.-M. Zhang, Y. Lu, W.-L. Chen and E.-B. Wang, *Chem. Eur. J.* 2014, **20**, 6927; (f) S. R. Bajpe, C. E. A. Kirschhock, A. Aerts, E. Breynaert, G. Absillis, T. N. Parac-Vogt, L. Giebeler and J. A. Martens, *Chem. Eur. J.*, 2010, **16**, 3926; (g) J. Song, Z. Luo, D. K. Britt, H. Furukawa, O. M. Yaghi, K. I. Hardcastle, and C. L. Hill, *J. Am. Chem. Soc.*, 2011, **133**, 16839; (h) J. J.-A. Alcañiz, M. Goesten, A. Martinez-Joaristi, E. Stavitski, A. V. Petukhov, J. Gascon and F. Kapteijn, *Chem. Commun.*, 2011, **47**, 8578. The complete list of references is given in the ESI section.
6. (a) J. H. Cavka, S. Jakobsen, U. Olsbye, N. Guillou, C. Lamberti, S. Bordiga and K. P. Lillerud, *J. Am. Chem. Soc.*, 2008, **130**, 13850; (b) M. J. Katz, Z. J. Brown, Y. J. Colón, P. W. Siu, K. A. Scheidt, R. Q. Snurr, J. T. Hupp and O. K. Farha, *Chem. Commun.*, 2013, **49**, 9449; (c) J. E. Mondloch, M. J. Katz, N. Planas, D. Semrouni, L. Gagliardi, J. T. Hupp and O. K. Farha, *Chem. Commun.*, 2014, **50**, 8944; (d) P. S. Barciá, D. Guimarães, P. A. P. Mendes, J. A. C. Silva, V. Guillerm, H. Chevreau, C. Serre and A. E. Rodrigues, *Microporous Mesoporous Mater.*, 2011, **139**, 67; (e) G. C. Schearer, S. Chavan, J. Ethiraj, J. G. Vitillo, S. Svelle, U. Olsbye, C. Lamberti, S. Bordiga and K. P. Lillerud, *Chem. Mater.*, 2014, **26**, 4068.
7. (a) F. Vermoortele, R. Ameloot, A. Vimont, C. Serre and D. De Vos, *Chem. Commun.*, 2010, **47**, 1521; (b) M. J. Katz, J. E. Mondloch, R. K. Totten, J. K. Park, S. T. Nguyen, O. K. Farha and J. T. Hupp, *Angew. Chem. Int. Ed.*, 2014, **53**, 497.
8. (a) S. Devautour-Vinot, C. Martineau, S. Diaby, M. Ben-Yahia, S. Miller, C. Serre, P. Horcajada, D. Cunha, F. Taulelle and G. Maurin, *J. Phys. Chem. C*, 2013, **117**, 11694; (b) J. He, J. Wang, Y. Chen, J. Zhang, D. Duan, Y. Wang and Z. Yan, *Chem. Commun.*, 2014, **50**, 7063; (c) C. Larabi and E. A. Quadrelli, *Eur. J. Inorg. Chem.* 2012, **18**, 3014.
9. A. Schaate, P. Roy, A. Godt, J. Lippke, F. Waltz, M. Wiebcke and P. Behrens, *Chem. Eur. J.*, 2011, **17**, 6643.
10. O. A. Kholdeeva, G. M. Maksimov, R. I. Maksimovskaya, M. P. Vanina, T. A. Trubitsina, D. Y. Naumov, B. A. Kolesov, N. S. Antonova, J. J. Carbó and J. M. Poblet, *Inorg. Chem.*, 2006, **45**, 7224.
11. (a) M. N. Sokolov, N. V. Izarova, E. V. Peresyphkina, D. A. Mainichev, and V. P. Fedin, *Inorg. Chim. Acta*, 2009, **362**, 3756; (b) S. Vanhaecht, G. Absillis and T. N. Parac-Vogt, *Dalton Trans.*, 2013, **42**, 15437.
12. R. J. Errington, P. S. S. Petkar, P. S. Middleton, and W. McFarlane, *J. Am. Chem. Soc.*, 2007, **129**, 12181.
13. (a) J. Chunjie, S. Shengnan, W. Xuyang, W. Xiangsheng, G. Hongchen, G. Xinwen and C. Lidong, *Acta Chim. Sinica*, 2013, **71**, 810; (b) S. Ribeiro, A. D. S. Barbosa, A. C. Gomes, M. Pillinger, I. S. Gonçalves, L. Cunha-Silva and S. S. Balula, *Fuel Process. Technol.*, 2013, **116**, 350.
14. G. Férey, C. Mellot-Draznieks, C. Serre, F. Millange, J. Dutour, S. Surblé and I. Margiolaki, *Science*, 2005, **309**, 2040.
15. P. M. Paes de Sousa, R. Grazina, A. D. S. Barbosa, B. de Castro, J. J. G. Moura, L. Cunha-Silva and S. S. Balula, *Electrochim Acta*, 2013, **87**, 853.